

Application of computer-aided drug repurposing in the search of new cruzipain inhibitors: discovery of amiodarone and bromocriptine inhibitory effects

Carolina L. Bellera¹, Darío E. Balcazar², Lucas Alberca¹, Carlos A. Labriola³, Alan Talevi^{1*}, Carolina Carrillo²

1.- Medicinal Chemistry, Department of Biological Sciences, Faculty of Exact Sciences, National University of La Plata, 47 y 115, La Plata (B1900AJI), Buenos Aires, Argentina. atalevi@biol.unlp.edu.ar, alantalevi@gmail.com

2.- Instituto de Ciencia y Tecnología Dr. César Milstein (ICT Milstein) – Argentinean National Council of Scientific and Technical Research (CONICET).

3.- Instituto de Investigaciones Bioquímicas de Buenos Aires - Argentinean National Council of Scientific and Technical Research (CONICET).

KEYWORDS. Chagas disease – computer- aided drug repurposing – drug repurposing – cruzipain – linear discriminant analysis

ABSTRACT: Cruzipain (Cz) is the major cystein protease of the protozoan *Trypanosoma cruzi*, etiological agent of Chagas disease. From a 163-compound dataset, a 2D-classifier capable of identifying Cz inhibitors was obtained and applied in a virtual screening campaign on the DrugBank database, which compiles FDA-approved and investigational drugs. 54 approved drugs were selected as candidates, 4 of which were acquired and tested on Cz and *T. cruzi* epimastigotes. Among them, the antiparkinsonian and antidiabetic drug bromocriptine and the antiarrhythmic amiodarone showed dose-dependent inhibition of Cz and antiproliferative activity on the parasite.

INTRODUCTION

Chagas disease (or American trypanosomiasis) is a tropical parasitic disease caused by the flagellate protozoan *Trypanosoma cruzi*. *T. cruzi* life-cycle includes both vertebrate (among them, man) and invertebrate (haematophagous triatomine bugs) hosts. Around 80-90% of infections in humans occur when the bug feces come into contact with wounded skin or mucosae¹. Other infection ways include blood-transfusion and congenital transmission. Even though a series of control campaigns (with an emphasis on vector control) undertaken by World Health Organization (WHO), Pan American Health Organization (PAHO) and national authorities have dramatically reduced Chagas disease prevalence in the last fifteen years, there are still almost 8 million infected people, 28 million people at risk and more than 40,000 annual new cases²⁻⁴.

Current treatment against Chagas relies on only two agents developed during 1960s-1970s, namely nifurtimox and benznidazole, which are not effective in the late chronic phase of the disease and present severe side-effects and resistance issues⁵⁻⁷. This explains why American trypanosomiasis has long been regarded as an orphan or neglected disease. It is worth noting, however, that important advances have been made in the field of biochemistry and molecular biology of *T. cruzi* and novel antichagasic therapeutics^{4, 8-11}. Cystein protease inhibitors are among the most investigated candidates against *T. cruzi*¹¹. Cruzipain (Cz), the major cystein protease of the parasite, has been particularly explored as new drug target. Cz is essential for replication of the intracellular form of *T. cruzi* and plays a role in host-parasite interactions¹². Since it is auto-

catalytic, it is believed that Cz inhibition produces accumulation of the inactive precursor of the proteinase within the Golgi complex, which eventually leads to osmotic shock and cell death¹³.

Here, we present the development of a 2D classification model from a 163-compound dataset which includes both Cz inhibitors and non-inhibitors. The model has later been applied in a virtual screening (VS) campaign to explore the DrugBank small molecule database in order to identify novel Cz reversible inhibitors. Four of the selected candidates were acquired and tested both biochemically and biologically, validating the model.

It is worth signaling that DrugBank compiles FDA-approved and experimental drugs (including biotech molecules and nutraceuticals)^{14,15}. It is therefore particularly useful to conduct VS campaigns aimed to drug repurposing (i.e. searching for second or further medical uses of known drugs). The application of VS to chemical libraries compiling known therapeutics can be considered as a form of knowledge-based, rational drug repositioning¹⁶⁻¹⁹, (chemoinformatics- and bioinformatics-based, and others) which has been recently signaled as a relevant strategy to aid discovering novel treatment for rare and neglected conditions²⁰⁻²².

RESULTS

Clustering procedure was applied on the dataset using a combination of Maximum Common Structure (MCS) hierarchical clustering and optimization by k-means clustering (see Experimental Section for details). Such procedure revealed 5 groups of at least 6

compounds in the ACTIVE category and 7 groups of at least 7 compounds in the INACTIVE class. According to MCS clustering, there are 4 compounds in the ACTIVE class which can be considered outliers (they are clustered alone or in groups of only two compounds, meaning they have no MCS above the specified number of atoms), whereas the INACTIVE category presents 14 outliers. On the basis of the clustering procedure, 25% of each cluster was assigned to the test set for external validation purposes, while the remaining 75% of each cluster were assigned to the training set upon which the model was derived.

The following model was obtained through Linear Discriminant Analysis (LDA):

$$\text{Class} = -0.959 + 1.764 \cdot \text{GGI7} - 0.287 \cdot \text{nS} + 0.280 \cdot \text{nCN}$$

$$\text{Wilks' } \lambda = 0.56 \quad F(3,117) = 31.24 \quad p < 0.0000$$

N=121

where GGI7 represents Galvez topological charge index of order 7, nS represents the number of sulfur atoms and nCN represents the number of aliphatic nitriles. The magnitudes of the beta coefficients of such descriptors are, in that order, 0.583, 0.183, 0.136, showing that GGI7 is the more relevant independent variable of the model. It should be highlighted that the model presents an excellent cases per predictor ratio (above 40) which indicates a very low chance of overfitting, as confirmed later in the external validation results. Furthermore the pairwise correlation between the descriptors included in the model is negligible, 0.147, being the correlation coefficient between the most correlated predictors. When using 0 as a score threshold to differentiate active from inactive compounds, the model presents 74% of good classifications among the training set inactive compounds, 80% of good classifications among the training set active compounds, and an overall of 77% good classifications. Regarding the test set, the model accurately classifies 81% of the active and 90.5% of the inactive compounds, with an overall good classification of 86%. These results seem to confirm that no overfitting has occurred, since the performance on the test set is similar to (and in fact, better than) the performance on the training set. The average performance of the randomized models was 63.6% (sd = 3.5) showing that the randomized models were significantly outperformed by the real model, as expected. The 24-fold cross-validation resulted in an average percentage of good-classifications of 77.6%, which is very similar to the performance of the original model on the training set.

We resorted to Pharmacological Distribution Diagrams (PDD) and Receiving Operating Characteristic (ROC) curves in order to optimize the chosen threshold score on a rational basis²³⁻²⁴. Figures 1 and 2 present, respectively, the PDD and training set ROC curve. The area under the curve (AUC) for the training and test sets ROC curves were, respectively, 0.893 and 0.921 (1 represents perfect classification, while 0.5 represents random classification). Note that the distribution of active and inactive compounds in relation to the model score are almost identical (Figure 1). It is also interesting to underline that 6 of the misclassified compounds (4 actives and 2 inactives) correspond to the ones identified as outliers

during the hierarchical clustering procedure (that is, compounds which do not share a 9-atom MCS with the rest). On the basis of the results, 0.29 was defined as cutoff value to differentiate active from inactive compounds in the VS campaign. According to the ROC curves data, this corresponds to a sensitivity of 67% and a specificity of 95% in the training set, and a sensitivity of 75% and a specificity of 100% in the test set. As stated by Triballeau in the original application of ROC curves to VS, the selection of a given balance between sensitivity and specificity is not a statistical matter but a context-dependent decision. In our case, due to a limited budget to acquire and test compounds, we have prioritized specificity (i.e. reducing the chance of false positives) over sensitivity. This means that potentially valuable active scaffolds will be loss during the screening, in order to reduce the chance of sending an inactive compound (false positive) to experimental testing.

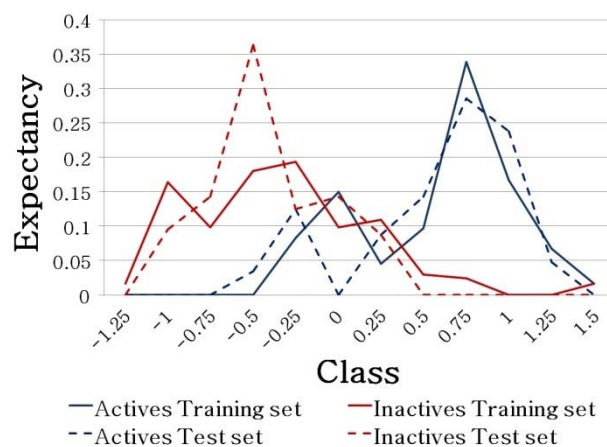


Figure 1. PDD showing the distribution of training and test set active and inactive compounds along the score values of the model. A fine superposition between training and test set is observed.

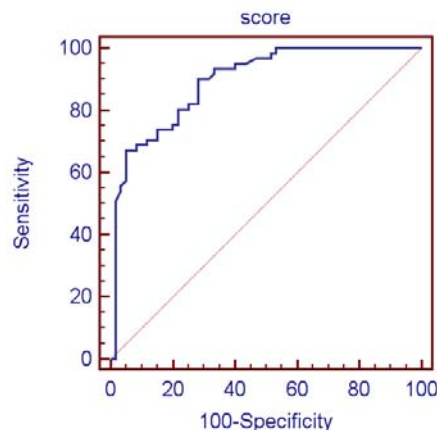


Figure 2. Training set ROC curve.

From 6684 small approved and investigational molecules of the DrugBank 3.0 database, 256 candidates belonging to the model's applicability domain presented a model score above the selected threshold; 54 of them correspond to approved drugs, which are the

straightforward candidates for repositioning purposes. On the basis of their accessibility, 4 of them (Figure 3) were acquired and experimentally tested in enzymatic assay on Cz crude extract. The acquired candidates were amiodarone (currently marketed as anti-arrhythmic), bromocriptine (approved as antiparkinsonian and antidiabetic), colchicine (gout treatment) and escitalopram (anti-depressant). Figure 4 shows the effect of 100 μM solutions of the four candidates on the Cz activity from *T. cruzi* crude extracts. Amiodarone and bromocriptine showed a significant inhibitory effect on Cz activity from cell extracts. Such inhibition proved to be dose-dependent on purified Cz (Figure 5), with a median inhibitory concentration (IC_{50}) approximately of 219,8 μM for amiodarone and 84,2 μM for bromocriptine

Both candidates also showed a notorious effect on *T. cruzi* epimastigotes proliferation (Figure 6) presenting values of median inhibitory dose (ID_{50}) around 22 μM for amiodarone and 15 μM for bromocriptine at the middle log phase of controls (4th day). The fact that amiodarone presents higher effects on epimastigotes culture than on Cz activity could be explained by a pleiotropic effect of the drug, as it has been previously showed on parasites' Ca^{2+} homeostasis and on ergosterol biosynthesis²⁵. Even though, it should be highlighted that this is the first time that the antitrypanosomal effect of amiodarone, at least partially, is related to Cz activity.

Bromocriptine showed a significant effect on parasite morphology (Figure 7) as well as amiodarone (not shown).

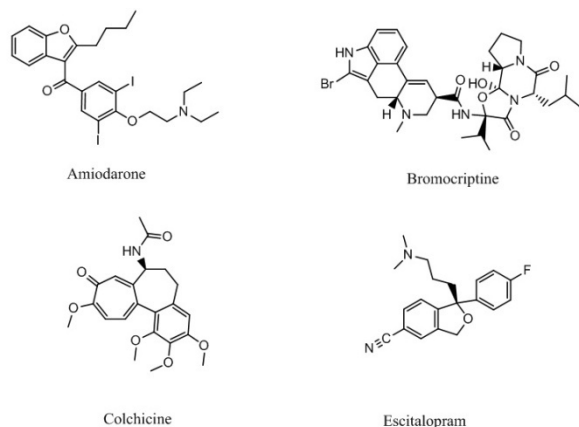


Figure 3. Molecular structures of the four candidates selected for enzymatic testing.

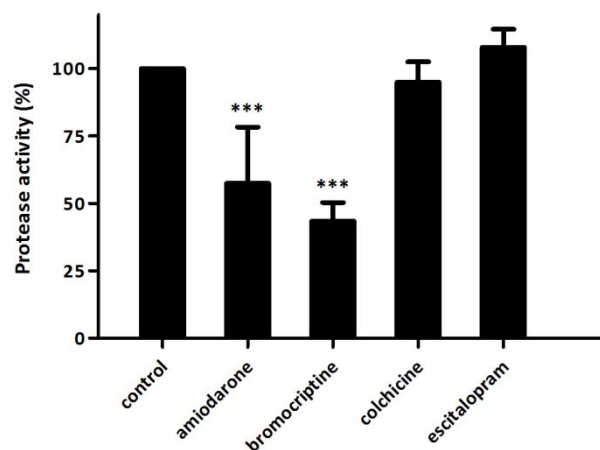


Figure 4. Inhibitory effect of the four selected candidates on Cz activity from *T. cruzi* crude extracts. The final concentration of each compound was 100 μM . Protease activity is expressed as percentage of the control condition (2% DMSO). Results represent the mean of three independent experiments. Asterisks indicate significant differences respect of the control (***) p < 0.005).

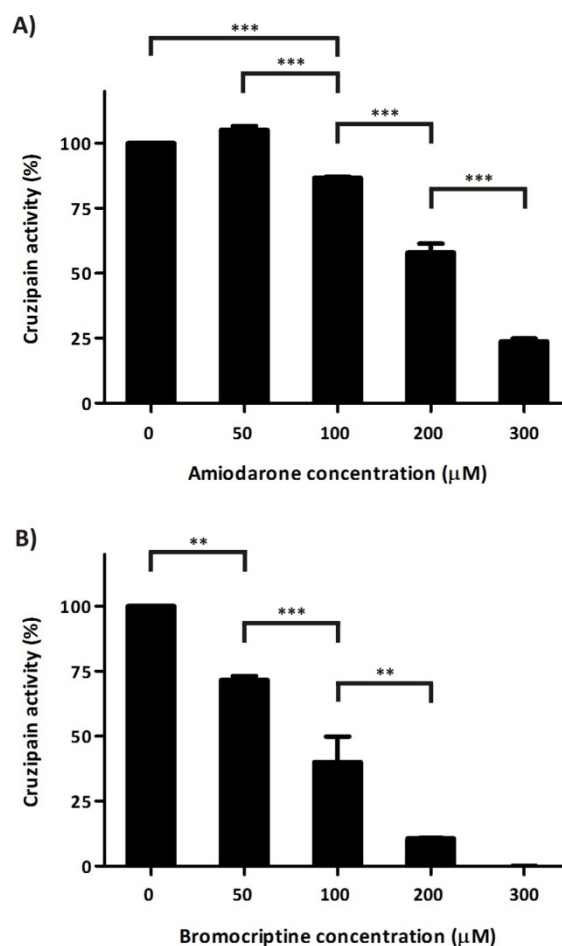


Figure 5. Dose-dependent inhibitory effect of amiodarone (A) and bromocriptine (B) on purified Cz activity. Both candidates were assayed in a concentration range of 0-300 μ M. Remanent Cz activity was expressed as a percentage of the control (0 μ M compound, 2% DMSO). Results represent the mean of two independent experiments. Asterisks indicate significant differences (** $p < 0.01$, *** $p < 0.005$).

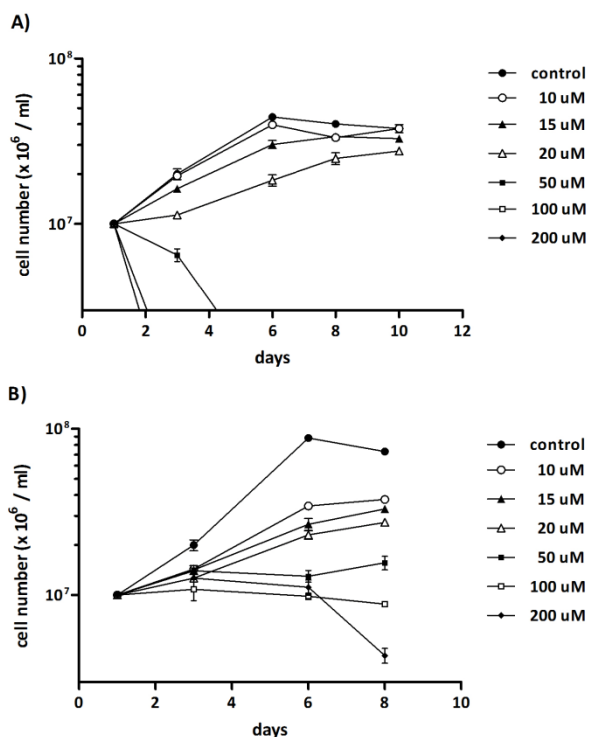


Figure 6. Effects on *T. cruzi* epimastigotes proliferation of (A) amiodarone and (B) bromocriptine. To determine the growth rate, 10⁷ cells/ml were seeded in BHT medium and maintained at 28°C for ten or eight days, respectively. The control condition was done with 2% DMSO. Parasites were counted using a hemocytometer chamber. Results represent the mean \pm SD of a representative experiment.

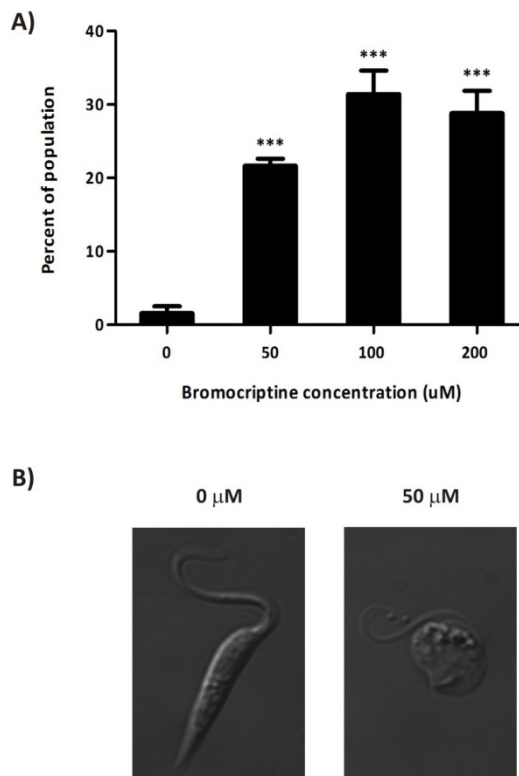


Figure 7. Effect of bromocriptine on *T. cruzi* morphology. A) Quantitation of morphological changes in cells that have been cultured in absence or presence of bromocriptine (50-200 μ M) for four days. At least 100 cells were counted for each condition classifying in normal and rounded parasites. Results represent the means of the two independent experiments. (***) $p < 0.005$, respect to 0 μ M). B) Differential interference contrast (DIC) photos of cells incubated for four days in presence (normal morphology) or absence (rounded morphology) of 50 μ M bromocriptine. Results represent images of an experiment representative.

DISCUSSION AND CONCLUSIONS

A 3-descriptor 2D classification model was derived from a 163-compound dataset which compiled Cz inhibitors and non-inhibitors extracted from literature. The model presented an excellent case to descriptor ratio and similar performance on both the training and the test sets, which suggest good predictive ability and absence of overfitting. Since only conformation-independent descriptors were included in the model, it is particularly suitable for efficient exploration of drug libraries through VS campaigns without requiring any preprocessing of the library structures.

Having in mind the potential of knowledge-based drug repositioning to develop novel drugs for neglected and rare diseases, the model was applied in a VS campaign to select potential antichagasic drugs from the DrugBank database, which compiles approved and investigational active ingredients. PDD and ROC curve analysis were conducted in order to select a score cutoff value to differentiate active and inactive agents on a rational basis.

Four candidates were acquired and experimentally tested in enzymatic and inhibitory assays. Among them, amiodarone (approved as antiarrhythmic) and bromocriptine (traditionally used against Parkinson and more recently repurposed for the treatment of diabetes) showed a weak but dose-dependent inhibition on Cz activity with clear effects on *T. cruzi* proliferation and morphology. The results illustrate the possibilities of computer-aided drug repositioning in the search of novel medications for neglected diseases.

It should be mentioned that two of the four candidates showed no or almost no activity on the enzyme, thus suggesting that either the model should be optimized or a stricter cutoff value should be selected to reduce the false positive rate (e.g. score above 0.5). As discussed by Triballeau et al. in the original application of ROC curves to VS campaigns²⁴, the probability of finding an active compound critically depends on the yield of active compounds of the screened database. The Positivity Predictive Value, which represents the probability that a given candidate with a score above the selected threshold will be actually active can be calculated through the following expression:

$$PPV = \frac{(Se)(Ya)}{(Se)(Ya) + (1 - Sp)(1 - Ya)}$$

where *Se* represents the sensitivity of the model (or true positives rate) and *Sp* represents the specificity of the model (or true negatives rate). *Ya* symbolizes the yield of actives, that is, the number of active drugs in the screened database divided by the total number of compounds in the database. *Ya* is not known in real VS applications. The influence of *Ya* on the probability that a given selected compound is actually active means that even a highly specific and sensitive model may retrieve a high proportion of false positives from a screened library if the yield of actives in the library is low. As it has been recently pointed out by Scior et al., the confirmed hit rate in VS real-world applications is often very low, between 0.01 and 0.14%²⁵. Noteworthy, if the selected cutoff value was 0.5, only bromocriptine among the four compounds would have overcome the screening and thus experimentally tested.

EXPERIMENTAL SECTION

Dataset compilation and splitting

A 163-compound balanced dataset including 82 Cz reversible inhibitors and 81 non-inhibitors was compiled from literature²⁶⁻³⁸. In order to split the dataset into representative training and test sets, the LibraryMCS v0.7 (ChemAxon) hierarchical clustering approach was applied in combination with the k-means clustering as implemented in Statistica 10 Cluster Analysis module (Statsoft Inc, 2011). LibraryMCS relies on the Maximum Common Substructure (MCS, i. e. the largest subgraph shared by two chemical graphs) to cluster a set of chemical structures. The algorithm applies a similarity search to the pool of molecules and the two structures with the highest similarity coefficient are considered more likely to share a large MCS. Once this likely MCS has been established, substructure search is carried out in order to find the MCS of multiple structures efficiently, without exhaustive pairwise comparison. Certainly, it is possible that the two structures exhibiting

the highest similarity coefficient do not share the largest MCS; thus, Library MCS leads to reproducible but approximate solutions³⁹. As suggested by Everitt et al.⁴⁰, hierarchical clustering has been applied here to define an initial partition of *n* objects into *g* groups, selecting a smallest common substructure of 9 atoms, and the groups of compounds were later optimized by k-means algorithm, minimizing the Euclidean distance to the group centers. A series of descriptors computed with Dragon 4.0 (Milano Chemometrics, 2003) representing different aspects of molecular structure (namely molecular weight, log P, polar surface area, number of H bonds acceptors, information index of atomic content, sum of atomic van der Waals volumes) were normalized and applied to calculate such distance. Once the clusters were separately identified in the inhibitors and non-inhibitors classes, 25% of each cluster was assigned to an independent test set for validation purposes, while the remaining 75% of the clusters were retained as training set for modeling purposes. The structures of both training and test set compounds are provided as Supplementary information.

Descriptor calculation and modeling

877 molecular 0D-2D molecular descriptors (constitutional and topological descriptors, functional group counts and atom-centered fragments) were computed with Dragon 4.0 Academic version. The values of such descriptors are conformation-independent, thus being particularly suitable for their application in VS campaigns, since no preprocessing of the database structures (e.g. conformational analysis or optimization) is required. From the 877 descriptors, 30 random subsets of no more than 254 descriptors were generated, and these subsets were used as descriptor pools for modeling purposes.

Linear Discriminant Analysis (LDA) was conducted in order to derive a classification model capable of distinguishing Cz inhibitors from non-inhibitors. LDA is a qualitative supervised learning method aimed to finding a linear combination of independent variables to discriminate between two or more categories of objects. Each object class is associated to a given value (an integer value) of an arbitrary variable that serves as class label. In our case, only two object classes (ACTIVE – Cz inhibitors, and INACTIVE – non-inhibitors) were considered, thus the class label assumes two observed values (1 and -1, respectively). Since the output of the function being searched is not a continuous variable but only an object category, LDA and other classificatory techniques may be useful to handle noisy data, e.g. if a given experimental endpoint is associated to large variability or if experimental data from a diversity of laboratories are compiled⁴¹.

The Discriminant Analysis module of Statistica 10 was used to derive the models. A tolerance value of 0.5 was selected in order to exclude highly correlated descriptors from the model. All the coefficients linked to the models descriptors were significant at a 0.05 level. A minimum ratio of 15 between the number of training set compounds and the number of independent variables was used in order to reduce the chances of overfitting. Parsimony principle, Wilks' lambda and the performance of the model on the test set were used to select the best model. Standard validation approaches (leave-group out cross-validation, Fisher's randomization test and external validation) were used to assess the model's robustness and

predictive ability⁴². Stratified 24-fold cross-validation and 55 randomization tests were applied.

Virtual Screening

DrugBank 3.0 was used for VS. Only approved and experimental small molecules and nutraceuticals (6684 total compounds) were considered (biotech drugs were excluded *a priori*). PDD and separate ROC curves were constructed for both the training and test sets, in order to select the discriminant function (score) threshold value to be used in the VS campaign²⁴. To build ROC curves MedCalc ROC curves analysis tool was used (Medcalc software, 2012). Finally, the leverage approach was used to define whether a given prediction belonged or not to the model's applicability domain⁴³. Briefly, the leverage for a compound *i* is defined as $h_i = x_i^T (X^T X)^{-1} x_i$, where x_i is the descriptor vector for compound *i* and *X* is the model matrix derived from the training set descriptor values. The warning leverage was fixed at $3k/n$, *k* being the number of model parameters and *n* the number of training set compounds.

Inhibitory effect on Cz activity assay

Four candidates from the VS were acquired and their ability to inhibit Cz was assessed. Amiodarone hydrochloride was a kind gift from Vannier Labs. Escitalopram oxalate was a kind gift from Bagó Labs. Bromocriptine and colchicine were acquired from Saporiti.

Parasite cultures were harvested, washed and incubated with lyses buffer (Hepes 50 mM pH 7.4, NaCl 200 mM, NP-40 1%). Cz activity from the extracts was assayed with 0.3 mM Bz-Pro-Phe-Arg-pNA (Bz-PFR-pNA) as substrate, as described previously⁴⁴. Briefly: a diluted aliquot from the cell extract was incubated in buffer 50 mM Tris-HCl pH 7.6, 5 μM Dithiothreitol (DTT) and 250 μM N-benzoyl N-Benzoyl-Pro-Phe-Arg-p-nitroanilide (Sigma), in presence or absence of the indicated compounds. The reaction was measured spectrophotometrically at room temperature, at 410 nm for 5 minutes (Beckman Coulter™ DU®530 Life Science UV/Vis Spectrophotometer.). The values obtained were converted into pmol of hydrolysed substrate per min by using the extinction coefficients 8.800 M⁻¹ cm⁻¹ (p-nitroanilides). The inhibitory effect of the selected candidates was expressed as a percentage of residual activity of Cz respect of the assay without inhibitors.

To confirm the specificity of the observed effect of bromocriptine on Cz activity, the enzyme was partially purified by ammonium sulfate precipitation followed by affinity column chromatography on concavalin A-sepharosa (Sigma), as previously described⁴⁵. The activity of the partially purified Cz was assayed using increasing bromocriptine concentrations

Inhibitory effects on growth curves of *T. cruzi* epimastigotes

Epimastigotes of the *T. cruzi* strain Y, were cultured at 28°C in BHT medium with 20mg/l Haemin, 20% heat-inactivated fetal calf serum and antibiotics (100 μg/ml streptomycin and 100 U/ml penicillin)⁴⁶, adding the indicated bromocriptine concentration (0 – 200uM).

Cultures were initiated at 10⁶ cells/ml and the proliferation was followed daily by cell counting in hemocytometer chamber.

For microscopy, freshly grown trypanosome samples were washed twice in PBS. After letting the cells settle for 30 min at room temperature in poly-L-lysine coated coverslips, parasites were fixed at room temperature for 20 min with 1% formaldehyde in PBS. Slides were mounted using Vectashield (Vector Laboratories). Cells were observed in an Olympus BX51 fluorescence microscope. Images were recorded with an Olympus XM10 camera.

The percent of rounded parasites was determined using an Zeiss Axiovert 25 microscope,

ASSOCIATED CONTENT

The compounds that compose the training and test sets are provided as Supplementary information. This material is available free of charge via the Internet at <http://pubs.acs.org>.

AUTHOR INFORMATION

Corresponding Author

* Alan Talevi, Faculty of Exact Sciences, National University of La Plata. 47 y 115, La Plata (B1900AJI), Buenos Aires, Argentina. atalevi@biol.unlp.edu.ar, alantalevi@gmail.com

Author Contributions

The manuscript was written through contributions of all authors. / All authors have given approval to the final version of the manuscript.

Funding Sources

This work was supported by the Faculty of Exact Sciences of the National University of la Plata, the National University of La Plata (UNLP), the Commission of Scientific Research of Buenos Aires Province (CIC) (PIRPS Projects and Incentivos UNLP), UBACyT - GF 20020100200029, University of Buenos Aires and PIP 2010 0685 from the National Council of Scientific and Technical Research (CONICET).

ACKNOWLEDGMENT

C. L. Bellera and D. Balcazar are fellowship holders from the National Council of Scientific and Technical Research (CONICET). C. Carrillo, C. Labriola and A. Talevi are members of CONICET. We are thankful to Bagó and Vannier for kindly providing samples of escitalopram and amiodarone, respectively.

ABBREVIATIONS

LDA, Linear Discriminant Analysis; MCS, Maximum Common Substructure; ROC, Receiving Operating Characteristic; VS, Virtual Screening.

REFERENCES

- [1] Rodrigues Coura, J.; de Castro, S. L. A critical review on Chagas disease chemotherapy. *Mem. Inst. Oswaldo Cruz* **2002**, 97, 3-24.
- [2] Moncayo, A.; Silveira, A. C. Current epidemiological trends for Chagas disease in Latin America and future challenges in epidemiology, surveillance and health policy. *Mem. Inst. Oswaldo Cruz* **2009**, 104 (Suppl. 1), 17-30.
- [3] World Health Organization. Control of Chagas disease. Second report of the WHO Expert Committee **2002**.
- [4] TDR (Special Programme for Research and Training in tropical diseases), World Health Organization. Research priorities for

Chagas disease, human African trypanosomiasis and leishmaniasis **2012**.

[5] Urbina, J. A.; Docampo, R. Specific chemotherapy of Chagas disease: controversies and advances. *Trends Parasitol.* **2003**, *19*, 495-501.

[6] Rodrigues Coura, J.; de Castro, S. L. A critical review on Chagas disease chemotherapy. *Mem. Inst. Oswaldo Cruz* **2002**, *97*, 3-24.

[7] Astelbauer, F.; Walochnik, J. Antiprotozoal compounds: state of the art and new developments. *Int. J. Antimicrob. Agents* **2011**, *38*, 118-124.

[8] Villalta, F.; Scharfstein, J.; Ashton, A. W.; Tyler, K. M.; Guan, F.; Mukherjee, S.; Lima, M. F.; Alvarez, S.; Weiss, L. M.; Huang, H.; Machado, F. S.; Tanowitz, H. B. Perspectives on the *Trypanosoma cruzi*-host cell receptor interactions. *Parasitol. Res.* **2009**, *104*: 1251-1260.

[9] Cuervo, P.; Domont, G. B.; De Jesus, J. B. Proteomics of trypanosomatids of human medical importance. *J. Proteomics.* **2010**, *73*, 845-867.

[10] Sánchez-Sancho, F.; Campillo, N. E.; Páez, J. A. Chagas disease: progress and new perspectives. *Curr. Med. Chem.* **2010**, *17*, 423-452.

[11] Duschak, V. G.; Couto, A. S. An insight on targets and patented drugs for chemotherapy of Chagas disease. *Recent Pat. Antiinfect. Drug Discov.* **2007**, *2*, 19-51.

[12] Duschak, V. G.; Couto, A. S. Cruzipain, the major cysteine protease for vaccine development and drug target. A review. *Curr. Med. Chem.* **2009**, *16*, 3174-3202.

[13] Rodrigues, G. C.; Aguiar, A. P.; da Silva Gonçalves Vianez, J. L.; Macrae, A.; de Melo, A. C. N.; Vermelho, A. B. Peptidase inhibitors as a possible therapeutic strategy for Chagas disease. *Curr. Enz. Inhib.* **2010**, *6*, 183-194.

[14] Knox, C.; Law, V.; Jewison, T.; Liu, P.; Ly, S.; Frolkis, A.; Pon, A.; Banco, K.; Mak, C.; Neveu, V.; Djoumbou, Y.; Eisner, R.; Guo, A. C.; Wishart D. S. DrugBank 3.0: a comprehensive resource for 'Omics' research on drugs. *Nucleic Acids Res.* **2011**, *39*, D1035-D1041.

[15] Wishart, D. S.; Knox, C.; Guo, A. C.; Stothard, S. P.; Chang, Z.; Woolsey, J. DrugBank: a comprehensive resource for *in silico* drug discovery and exploration. *Nucleic Acid Res.* **2006**, *34*, D668-D672.

[16] Glan, F.; Cao, B.; Wu, D.; Chen, Z.; Hou, T.; Mao, X. Exploring old drugs for the treatment of hematological malignancies. *Curr. Med. Chem.* **2011**, *18*, 1509-1514.

[17] Talevi, A.; Castro, E. A.; Bruno-Blanch, L. E. Virtual screening: an emergent, key methodology for drug development in an emergent continent – A bridge towards patentability. In *Advances Methods and Applications in Chemoinformatics: Research Progress and New Applications*, 1st ed.; Castro, E. A., Haghi, A. K., Eds.; IGI Global: Hershey, 2011; pp. 229-246.

[18] Deftereos, S. N.; Andronis, C.; Friedla, E. J.; Persidis, A.; Persidis, A. Drug repurposing and adverse event prediction using high-throughput literature analysis. *Wiley Interdiscip. Rev. Sys. Biol.* **2011**, *3*, 323-334.

[19] Lussier, Y. A.; Chen, J. L. The emergence of genome-based drug repositioning. *Sci. Transl. Med.* **2011**, *3*, 96ps35.

[20] Ekins, S.; Williams, A. J.; Krasowski, M. D.; Freundlich, J. S. *In silico* repositioning of approved drugs for rare and neglected diseases. *Drug Discov. Today* **2011**, *16*, 298-310.

[21] Sardana, A.; Zhu, C.; Zhang, M.; Gudivada, R. C.; Yang, L.; Jegga, A. G. Drug repositioning for orphan diseases. *Brief. Bioinform.* **2011**, *12*, 346-356.

[22] Pollastri, M. P.; Campbell, R. K. Target repurposing for neglected diseases. *Future Med. Chem.* **2011**, *3*, 1307-1315.

[23] Gálvez, J.; García-Domenech, R.; Alapont de Gregorio, C.; de Julián-Ortiz, J. V.; Popa, L. Pharmacological Distribution Diagrams: a tool for *de novo* drug design. *J. Mol. Graph.* **1996**, *14*, 272-276.

[24] Triballeau, N.; Acher, F.; Brabet, I.; Pin, J. P.; Bertrand, H. O. Virtual screening workflow development guided by the "Receiver Operating Characteristic" curve approach. application to high-throughput docking on metabotropic glutamate receptor subtype 4. *J. Med. Chem.* **2005**, *48*, 2534-2547.

[25] Benaim, G.; Sanders, J. M.; García-Marchán, Y.; Colina, C.; Lira, R.; Caldera, A. R.; Payares, G.; Sanoja, C.; Burgos, J. M.; Leon-Rossell, A.; Concepción, J. L.; Schijman, A. G.; Levin, M.; Oldfield, E.; Urbina, J. A. Amiodarone has intrinsic anti-*Trypanosoma cruzi* activity and acts synergistically with posaconazole- *J. Med. Chem.* **2006**, *49*, 892-899.

[26] Bender, A.; Tresadern, G.; Medina-Franco, J. L.; Martínez-Mayorga, K.; Langer, T.; Cuanalo-Contreras, K.; Agrafiotis, D. K. Recognizing pitfalls in virtual screening: a critical review. *J. Chem. Inf. Model.* **2011**, *52*, 867-881.

[27] dos Santos Filho, J. M.; Lima Leite, A. C.; Galdino de Oliveira, B.; Magalhães Moreira, D. R.; Lima, M. S.; Pereira Soares, M. B.; Leite, L. F. C. C. Design, synthesis and cruzain docking of 3-(4-substituted-aryl)-1,2,4-oxadiazole-N-acylhydrazones as anti-*Trypanosoma cruzi* agents. *Bioorg. Med. Chem.* **2009**, *17*, 6682-6691.

[28] Zaldini Hernandez, M.; Montenegro Rabello, M.; Lima Leite, A. C.; Oliveira Cardoso, M. V.; Magalhães Moreira, D. R.; Brondani, D. J.; Simone, C. A.; Campos Reis, L.; Assis Souza, M.; Alves Pereira, V. R.; Salgado Ferreira, R.; McKerrow, J. H. Studies toward the structural optimization of novel thiazolyldiazone-based potent antitrypanosomal agents. *Bioorg. Med. Chem.* **2010**, *18*, 7826-7835.

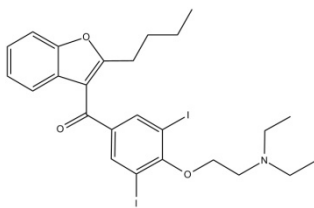
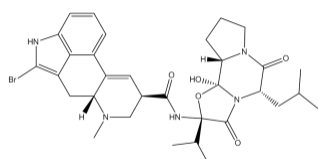
[29] Rodrigues, C. R.; Flaherty, T. M.; Springer, C.; McKerrow, J. H.; Cohen, F. E. CoMFA and HQSAR of acylhydrazide cruzain inhibitors. *Bioorg. Med. Chem. Lett.* **2002**, *12*, 1537-1541.

[30] Huang, L.; Brinen, L. S.; Ellman, J. A. Crystal structures of reversible ketone-based inhibitors of the cysteine protease cruzain. *Bioorg. Med. Chem.* **2003**, *11*, 21-29.

[31] Choe, Y.; Brinen, L. S.; Price, M. S.; Engel, J. C.; Lange, M.; Grisostomi, C.; Weston, S. G.; Pallai, P. V.; Cheng, H.; Hardy, L. W.; Hartsough, D. S.; McKain, M.; Tilton, R. F.; Baldino, C. M.; Craik, C. S. Development of α -keto-based inhibitors of cruzain, a cysteine protease implicated in Chagas disease. *Bioorg. Med. Chem.* **2005**, *13*, 2141-2156.

- [32] Beaulieu, C.; Isabel, E.; Fortier, A.; Massé, F.; Mellon, C.; Méthot, N.; Ndao, M.; Nicoll-Griffith, D.; Lee, D.; Park, H.; Black, W. C. Identification of potent and reversible cruzipain inhibitors for the treatment of Chagas disease. *Bioorg. Med. Chem. Lett.* **2010**, *20*, 7444-7449.
- [33] Du, X.; Hansell, E.; Engel, J. C.; Caffrey, C. R.; Cohen, F. E.; McKerrow, J. H. Aryl ureas represent a new class of anti-trypanosomal agents. *Chem. Biol.* **2000**, *7*, 733-742.
- [34] Brak, K.; Doyle, P. S.; McKerrow, J. H.; Ellman, J. A. Identification of a new class of nonpeptidic inhibitors of cruzain. *J. Am. Chem. Soc.* **2008**, *130*, 6404-6410.
- [35] Mott, B. T.; Ferreira, R. S.; Simeonov, A.; Jadhav, A.; Kean-Ang, K. K.; Leister, W.; Shen, M.; Silveira, J. T.; Doyle, P. S.; Arkin, M. R.; McKerrow, J. H.; Inglese, J.; Austin, C. P.; Thomas, C. J.; Shoichet, B. K.; Maloney, D. J. Identification and optimization of inhibitors of trypanosomal cysteine protease: cruzain, rhodesain, and TbCatB. *J. Med. Chem.* **2010**, *53*, 52-60.
- [36] Ferreira, R. S.; Simeonov, A.; Jadhav, A.; Eidam, O.; Mott, B. T.; Keiser, M. J.; McKerrow, J. H.; Maloney, D. J.; Irwin, J. J.; Shoichet, B. K. Complementarity between a docking and a high-throughput screen in discovering new cruzain inhibitors. *J. Med. Chem.* **2010**, *53*, 4891-4905.
- [37] Ang, K. K. H.; Ratnam, J.; Gut, J.; Legac, J.; Hansell, E.; Mackey, Z. B.; Skrzypczynska, K. M.; Debnath, A.; Engel, J. C.; Rosenthal, P. J.; McKerrow, J. H.; Arkin, M. R.; Renslo, A. R. Mining a Cathepsin Inhibitor Library for New Antiparasitic Drug Leads. *PLoS Negl. Trop. Dis.* **2011**, *5*, e1023.
- [38] Scheidt, K. A.; Roush, W. R.; McKerrow, J. H.; Selzer, P. M.; Hansell, E.; Rosenthal, P. J. Structure-based design, synthesis and evaluation of conformationally constrained cysteine protease inhibitors. *Bioorg. Med. Chem.* **1998**, *6*, 2477-2494.
- [39] Hariharan, R.; Janakiraman, A.; Nilakantan, R.; Singh, B.; Varghese, S.; Landrum, G.; Schuffenhauer, A. MultiMCS: a fast algorithm for the maximon common substructure problem on multiple molecules. *J. Chem. Inf. Model.* **2011**, *51*, 788-806.
- [40] Everitt, B. S.; Landau, S.; Leese, M.; Stahl, D. Optimization clustering techniques. In *Cluster Analysis*, 5th ed.; Balding, D. J., Cressie, N. A. C., Fitzmaurice, G. M., Goldstein, H., Molenberghs, G., Scott, D. W., Smith, A. F. M., Tsay, R. S., Weisberg, S., Eds.; John Wiley & Sons: Chichester, **2011**; pp. 111-142.
- [41] Talevi, A.; Bellera, C. L.; Di Ianni, M. E.; Duchowicz, P. R.; Bruno-Blanch, L. E.; Castro, E. A. An integrated drug development approach applying topological descriptors. *Curr. Comput-Aid. Drug.* **2012**, *8*, 172-181.
- [42] Yasri, A.; Hartsough, D. Toward an optimal procedure for variable selection and QSAR model building. *J. Chem. Inf. Comp. Sci.* **2001**, *41*, 1218-1227.
- [43] Tropsha, A.; Gramatica, P.; Gombar, V. The importance of being earnest: validation is the absolute essential for successful application and interpretation of QSPR models. *QSAR Comb. Sci.* **2003**, *22*, 69-77.
- [44] Cazzulo, J. J., M. C. Cazzulo Franke, J. Martinez, and B. M. Franke de Cazzulo. 1990. Some kinetic properties of a cysteine proteinase (Cruzipain) from *Trypanosoma cruzi*. *Biochim. Biophys. Acta.* **1037**:186-191
- [45] Labriola C, Sousa M, Cazzulo JJ. *Biol Res.* **1993**;26(1-2):101-7. Purification of the major cysteine proteinase (cruzipain) from *Trypanosoma cruzi* by affinity chromatography.
- [46] Cazzulo, J. J., B. M. Franke de Cazzulo, J. C. Engel, J. J. Cannata. 1985. End products and enzyme levels of aerobic glucose fermentation in trypanosomatids. *Mol. Biochem. Parasitol.* **16**:329-343.

TOC Graphic



0 μ M



50 μ M

